

## Unraveling the Structure and Dynamics of Excitons in Semiconductor Quantum Dots

PATANJALI KAMBHAMPATI\*

Department of Chemistry, McGill University, Montreal, QC H3A 2K6, Canada

RECEIVED ON MARCH 11, 2010

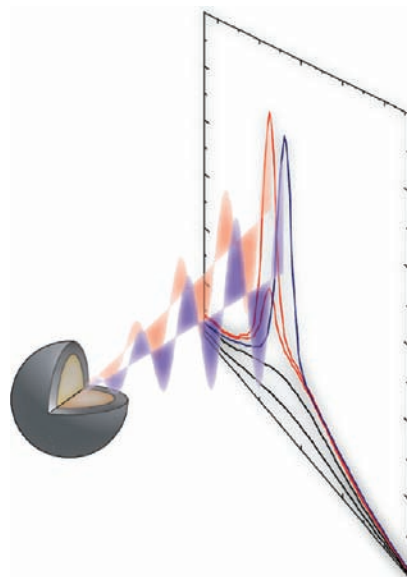
### CONSPECTUS

The quantum dot, one of the central materials in nanoscience, is a semiconductor crystal with a physical size on the nanometer length scale. It is often called an “artificial atom” because researchers can create nanostructures which yield properties similar to those of real atoms. By virtue of having a size in between molecules and solids, the quantum dot offers a rich palette for exploring new science and developing novel technologies.

Although the physical structure of quantum dots is well known, a clear understanding of the resultant electronic structure and dynamics has remained elusive. However, because the electronic structure and dynamics of the dot, the “excitonics”, confer its function in devices such as solar cells, lasers, LEDs, and nonclassical photon sources, a more complete understanding of these properties is critical for device development. In this Account, we use colloidal CdSe dots as a test bed upon which to explore four select issues in excitonic processes in quantum dots. We have developed a state-resolved spectroscopic approach which has yielded precise measurements of the electronic structural dynamics of quantum dots and has made inroads toward creating a unified picture of many of the key dynamic processes in these materials.

We focus on four main topics of longstanding interest and controversy:

(i) hot exciton relaxation dynamics, (ii) multiexcitons, (iii) optical gain, and (iv) exciton–phonon coupling. Using this state-resolved approach, we reconcile long standing controversies related to phenomena such as exciton cooling and exciton–phonon coupling and make surprising new observations related to optical gain and multiexcitons.



### 1. Overview of Excitonics in Quantum Dots

The semiconductor quantum dot has been under intense investigation both as a rich platform for basic science and for its promise in a wide variety of emerging technologies. The key feature of these materials is that they are physically intermediate between the limit of molecules and bulk solids.<sup>1–4</sup> Being in this regime, the quantum dot is one of the canonical systems of nanoscience.

While the rich variety of *physical* structures easily offer a clear avenue of interest and science, there is also a less obvious and possibly more sig-

nificant aspect to the quantum dot: their *electronic* structure. The elementary excitation in these systems is an *exciton*, comprising a bound electron–hole pair. Physical confinement of the charge carriers is well-known to yield quantum confinement effects, a point which can *qualitatively* be understood in terms of the simple particle in a sphere picture.<sup>5</sup>

Despite its intuitive appeal, this qualitative picture misses the vast majority of the underlying properties of the material. It is the real electronic structure and dynamics which confers the *function* of these materials. The quantum dot holds

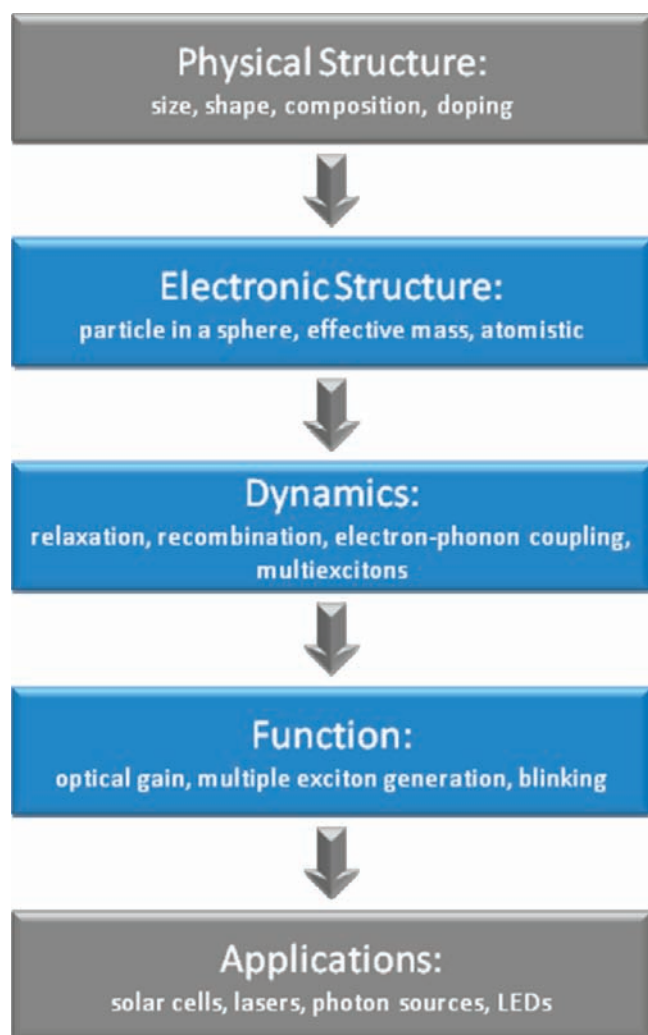


**FIGURE 1.** Relating the more transparent issues of physical structure and applications to the more abstract issues of electronic structure and dynamics.

promise for a wide variety of applications including energy efficient light emitting diodes, lasers, solar cells, single photon sources, and entangled photon sources.<sup>1,3,4,6</sup> Each of these applications is intimately connected to the electronic structural dynamics of the dot, its *excitonics*. Figure 1 illustrates the relationship between the physical structure of nanoscale materials and their implementation into devices: the structure and dynamics of excitons.

In this Account, we discuss four key topics in the excitonics of quantum dots: hot exciton relaxation dynamics, exciton–exciton interactions, optical gain, and exciton–phonon interactions. Other topics such as multicarrier recombination<sup>3,4</sup> and its reverse process of multiple exciton generation (MEG)<sup>3</sup> are not explicitly discussed here. Both, however, are intimately connected to the processes discussed here. In conjunction with electronic structure of the exciton, these topics represent the pathway to understanding the work-

ings of the quantum dot. We have developed a *state-resolved* spectroscopic approach<sup>7</sup> which has yielded precision measurements of the electronic structural dynamics,<sup>8–16</sup> and has ultimately made inroads toward creating a unified picture of many of the key dynamical processes in these materials.

## 2. State-Resolved Spectroscopy of Excitons in Quantum Dots

The semiconductor quantum dot is the best studied of the nanostructured materials. It offers a case study for many of the principles which can be generalized toward other nanostructured materials. The simplest picture of the quantum dot is the *particle-in-a-sphere*. This picture enables one to qualitatively understand the size tunable absorption spectrum and the existence of discrete features in the absorption spectrum. However, this simple picture misses much of the tremendous richness and complexity of these systems. Hence, it is important to note the *hierarchies* of theory necessary to understand aspects of the excitonics of quantum dots. In many cases, a higher level of theory does not merely produce a more precise number, but can *qualitatively* change the basic understanding of some observable.

The main levels of theory are particle-in-a-sphere (PIS),<sup>5</sup> multiband effective mass approximation (EMA) approach,<sup>2,17</sup> and atomistic approaches such as empirical pseudopotential method (EPM)<sup>18</sup> and *ab initio*.<sup>19</sup> The PIS approach provides no insight into many of the simplest aspects of the dot, such as the fluorescence Stokes shift<sup>20</sup> or the nature of the excitonic transitions in the absorption spectrum.<sup>15,17,21</sup> Hence, the minimal level of theory required to design and interpret these experiments is the EMA approach. EMA has been applied to these colloidal CdSe quantum dots by Efros, Bawendi, and Norris.<sup>2,17,20</sup> Those studies have yielded tremendous insight into the electronic structure and linear optical properties of these materials. These EMA results have furthermore informed the design and much of the interpretation of our experiments<sup>7–16</sup> summarized here. We note, however, that the atomistic (whether EPM<sup>18,21</sup> or *ab initio*<sup>19</sup>) approaches often yield *qualitatively* different results (e.g., ordering of states, bright/dark states, piezoelectricity, exciton cooling). Hence, the level of theory used to understand the observables is quite important.

Figure 2b shows a representative absorption spectrum of colloidal CdSe quantum dots. One can clearly see transitions which can be assigned to specific excitonic states (based upon the level of theory used). Also shown are laser spectra tuned in resonance to these excitonic states in order to perform exci-

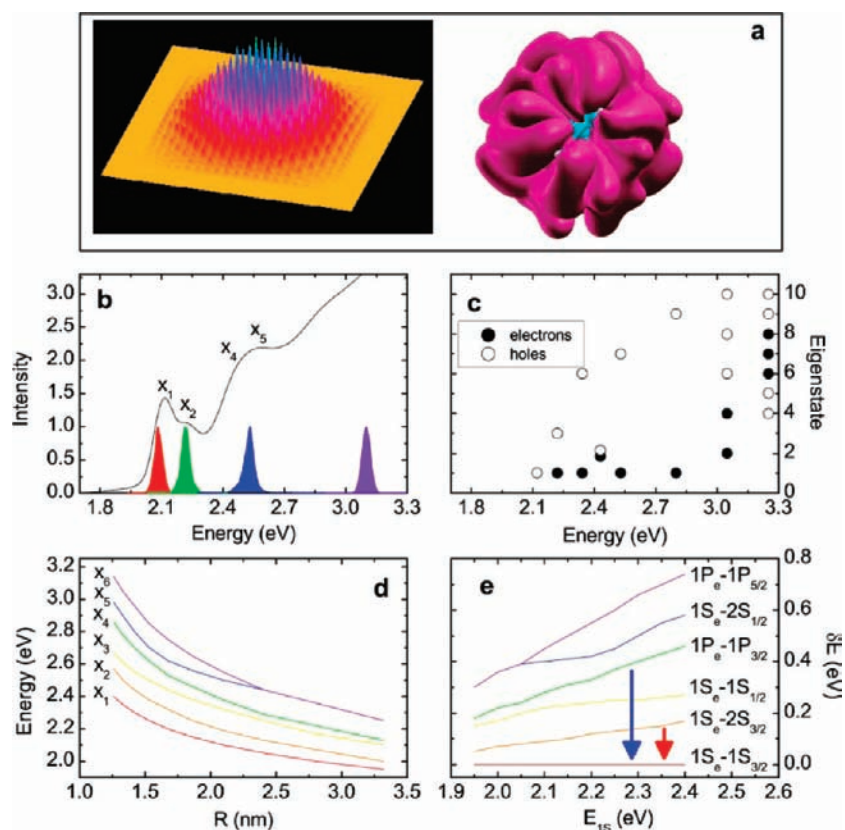


**FIGURE 2.** Illustration of the manifold of excitonic states and the manner in which one can spectroscopically probe dynamical processes with state-specificity. (a) Representative of atomistic wave functions of a GaAs quantum dot (LUMO, left) and Si quantum dot (exciton, right), courtesy of A. Franceschetti and O. Prezhdo, respectively. (b) Absorption spectrum of CdSe quantum dot and representative pump spectra used. (c) Excitonic states as a function of energy in the EMA picture. (d) The manifold of states vs radius. (e) The states vs  $X_1$  energy (adapted from ref 17).

tonic *state-resolved spectroscopy*, the focus of this Account. Figure 2c–e shows the manifold of excitonic states for this size of dot, and size-dependent energies of the manifold of states. The states denoted here are within the EMA approach.<sup>1,2,7–9,17</sup> The main point is that the lower excitonic states are quantized. As the energy increases, the density of states increases and ultimately converges toward a continuum.

Given the existence of quantized excitonic eigenstates, one anticipates the possibility of exploiting these discrete transitions to probe processes with excitonic *state-selectivity*. An obvious use of such a state-resolved approach is in the evaluation of exciton cooling.<sup>6</sup> The topic of hot exciton relaxation (cooling) is in the same vein as molecular work such as radiationless transitions. One aims to obtain a precision measurement of some relaxation process and to relate this measurement to a clear picture of the factors which govern the dynamics.

This goal of measuring a *well-specified* relaxation process becomes complex once one notes the manifold of excitonic states, which in some cases can go from *hot* electron to *cold* electron as excitonic energy increases (Figure 2c).<sup>2,7–9,17</sup> Using

femtosecond pump/probe spectroscopy, one can prepare some initially hot excitonic state and monitor its relaxation to the band edge exciton using a time delayed probe pulse. In the absence of state-selectivity, however, the initial state may be highly excited.<sup>4</sup> Hence the relaxation process measured would correspond to a complex set of sequential kinetics,<sup>7–9</sup> for example,  $X_5 \rightarrow X_4 \rightarrow X_3$  and so on. In this situation, it would be impossible to *unambiguously* extract a size-dependent transition rate for a key process, for example,  $1P \rightarrow 1S$  electron relaxation.

Our state-resolved approach<sup>7–9</sup> employs *tunable* femtosecond pulses in which the pump and probe pulses are tuned into *specific* transitions in order to cleanly extract the dynamics of interest. For example, the red laser spectrum (Figure 2b) corresponds to the electronically cold, band edge exciton ( $X_1$ ). Employing a green or blue laser spectrum pumps the system into different excitons comprising either a hot hole ( $X_2$ ) or a hot electron ( $X_4$ ) (Figure 2d,e). Hence, tuning the pump pulse to specific transitions suggests the possibility of monitoring electron or hole relaxation dynamics with excitonic *state-specificity*.

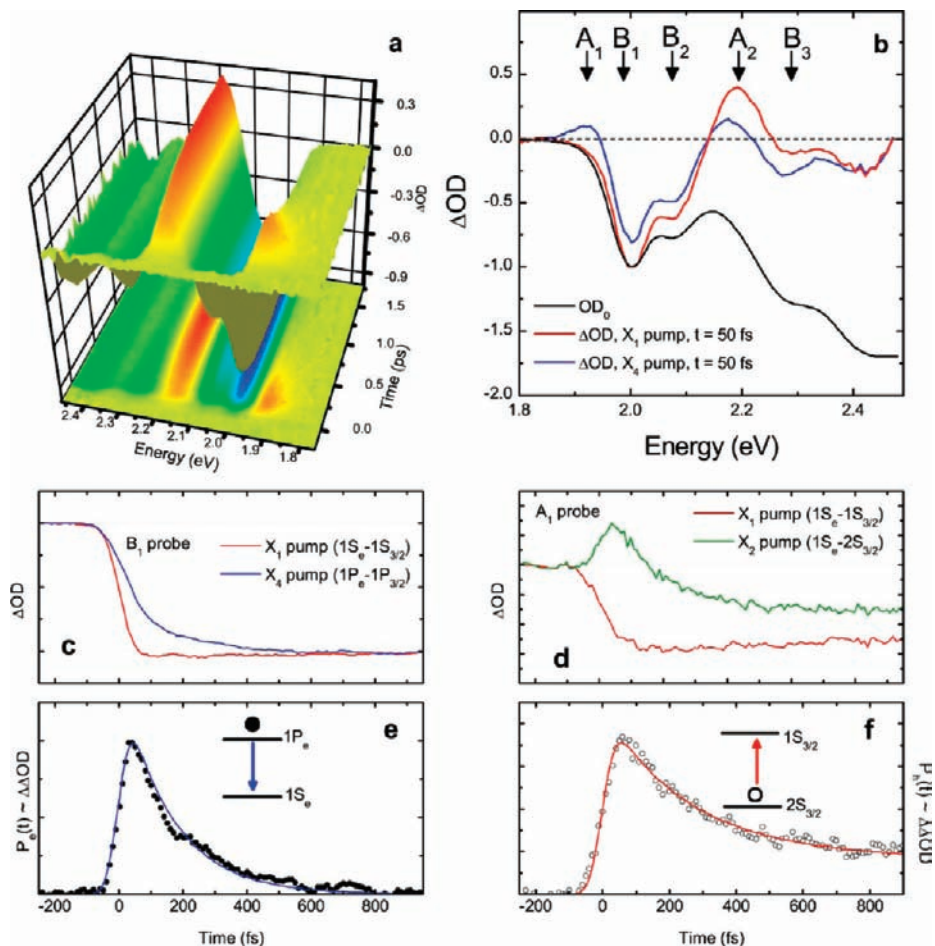


**FIGURE 3.** Illustration of state-resolved exciton dynamics via femtosecond pump/probe spectroscopy. (a) Time-resolved transient absorption (TA) spectrum upon excitation into  $X_4$  ( $1P_e-1P_{3/2}$ ). (b) TA spectrum upon excitation into  $X_1$  and  $X_4$  at  $t = 50$  fs. There are regions of induced absorptions ( $A_i$ ) and bleaches ( $B_i$ ). (c) Pump/probe transients upon excitation into two different initial excitonic states and probing the  $B_1$  spectral feature. (d) Pump/probe transients upon excitation into two different initial excitonic states and probing the  $A_1$  spectral feature. (e) Subtraction of the  $B_1$  transients directly monitors  $1P \rightarrow 1S$  electron relaxation. (f) Subtraction of the  $A_1$  spectral feature directly monitors the  $2S_{3/2} \rightarrow 1S_{3/2}$  hole relaxation.

The results of this *state-resolved* approach are summarized in Figure 3. The pump/probe or time-resolved transient absorption (TA) spectrum reveals rich dynamics (Figure 3a). A TA spectrum at various points in time (Figure 3b) enables further inspection of the sources of the optical nonlinearities. These nonlinearities (e.g., state-filling and level shifting) have been discussed at length in excellent reviews by Klimov.<sup>1,4</sup> The main difference in our experiments is that one can now pump *directly* into specific initial states by virtue of tunable femtosecond optical parametric amplifiers. The TA spectra in Figure 3b reveal clear differences in the bleaching ( $B_1$ ,  $B_2$ , etc.) and absorptive ( $A_1$ ,  $A_2$ , etc.) signals based upon initial excitonic state.

The probed spectral region can be judiciously selected to reveal *specific* dynamical processes. For example, the  $B_1$  feature arises from state-filling of the  $1S$  electron level.<sup>1,4,7-9</sup> Hence the *differences* in the  $B_1$  transients (Figure 3c and e)

reflect electron relaxation dynamics. Similarly, the  $A_1$  spectral feature reflects the charge distribution of the exciton. Hence, in a situation in which the *electron* is in the same state ( $X_1$  and  $X_2$ ), the differences in the  $A_1$  transient (Figure 3d and f) reflect hole relaxation dynamics.<sup>7-9</sup>

By judicious choice in the initially pumped excitonic state and the spectral feature probed, one is now able to reduce a many-level system to an *effective* two-level system. In doing so, we recover the ability to monitor hot exciton relaxation dynamics with excitonic state-to-state specificity for the first time.<sup>7-9</sup> The main result is that we can measure well-specified population dynamics corresponding to transitions from the first excited state to the lowest state for both electrons (Figure 3e) and holes (Figure 3f). This approach was also used to probe a wide variety of other fundamental properties of excitons in quantum dots.<sup>10-16</sup>

### 3. Hot Exciton Relaxation Dynamics

One of the longest standing and most important topics in quantum dot science is the issue of hot exciton cooling.<sup>4,6–9,22–24</sup> The question is seemingly simple: what are the time scales and pathways of hot carrier (electron and/or hole) relaxation to their lowest energy states (band edge exciton)?

The interest in this topic arises naturally from fundamental questions of the nature of the quantum confinement effect. To what extent does quantum confinement perturb relaxation pathways and possibly create new ones? The motivation for answering this question also arises from its importance in laying out the design principles for quantum dot based optoelectronic devices.<sup>4,6,23</sup> For example, one may require fast intraband relaxation for interband lasers and slow relaxation for interband lasers.<sup>23,24</sup> These relaxation processes also impact the science of quantum dot solar cells as these cooling processes can control and compete with processes such as multiple exciton generation (MEG) and hot carrier extraction.

This question arose historically from semiconductor physics research into hot carrier relaxation. In bulk semiconductors, there is a continuous energy spectrum. The electronic states can dissipate energy and cool via emission of phonons.<sup>3,4,6</sup> The electronic continuum ensures conservation of energy and thus a fast relaxation rate. Since quantum dots have a quantized spectrum with energy gaps (50–200 meV) greatly exceeding phonon energies (acoustic  $\sim 2$  meV, optical  $\sim 20$  meV), one anticipates that the carrier cooling will be much slower due to the requirement of multiphonon emission. This anticipated slowing of relaxation is called the “phonon bottleneck”.<sup>4,6–9,19,23,24</sup> Figure 4a illustrates the electronic relaxation problem for molecules, quantum dots, and bulk semiconductors. In molecules, one has a small number of electronic states ( $S_1$ ,  $T_1$ ) that are dressed with vibronic progressions (shown). In quantum dots, there are many excitonic states (shown) as well as vibronic progressions and single/triplet type fine structure (not shown). And in bulk solids, one finds an electronic continuum. This continuum is also found at higher energies in quantum dots.

Answering this question both experimentally<sup>4,6,23,24</sup> and theoretically<sup>22,25</sup> has proven to be quite challenging. The difficulty arises from the complex electronic structural dynamics in the dots: their excitonics. Investigations into electron cooling ( $1P \rightarrow 1S$ ) in high quality colloidal CdSe quantum dots was first done in pioneering work by Klimov.<sup>4</sup> They found that as the dots became smaller and the energy gaps larger, the electron cooling rates *increased*, in direct opposition to expect-

tations from the phonon bottleneck picture. Those results could be rationalized in terms of a new confinement mediated relaxation channel in quantum dots: the Auger relaxation channel proposed by Efros et al.<sup>22</sup> In related work, Guyot-Sionnest et al. showed that electron cooling is greatly slowed upon spatially decoupling the hole.<sup>24</sup> In this scenario, the electron cooling rate was sensitive to the surface ligands, thereby suggesting some ligand based relaxation channel. Throughout these experimental and theoretical investigations, a clear understanding of the time scales and pathways of the relevant processes had remained elusive.

From an experimental standpoint, the main difficulty arose from the complex manifold of excitonic states.<sup>7,9,17</sup> This manifold renders it impossible to *quantitatively* measure relaxation rates between well specified initial and final states, for all sizes of dots. In order to circumvent this problem, we introduced a *state-resolved* femtosecond spectroscopic approach to measuring electron and hole relaxation dynamics.<sup>7–9</sup> In this approach, we use a femtosecond pump pulse to *directly* excite into the first excited state of the electron or hole. Doing so forces each carrier to undergo transitions from a well specified initial state to a well specified final state, bypassing the manifold problem. Second, judicious choice in the probe spectrum enabled us to monitor electron relaxation or hole transition rates (survival probabilities) in isolation.<sup>7–9</sup>

The results of these measurements are summarized in Figure 4b,c. Figure 4b shows the size-dependent upper state lifetimes for electrons ( $1P \rightarrow 1S$ ) and holes ( $2S_{3/2} \rightarrow 1S_{3/2}$ ), in the EMA picture. Figure 4c recasts the data in terms of energy loss rate as a function of energy gap. This representation most clearly reveals the presence or absence of a carrier relaxation bottleneck. These state-resolved measurements of *electron* relaxation are consistent with the earlier work of Klimov.<sup>4</sup> By virtue of measuring a well-specified state-to-state transition process, these results provide the first *quantitative* measure of a well specified *transition process* rather than a qualitative estimate of cooling. Hence, these results significantly extend the earlier work, adding the precision required as a test of theory.

The more remarkable result is the complete absence of a phonon bottleneck for *holes*. The underlying premise is that the ultrafast Auger relaxation channel unidirectionally transfers energy from the electron to the hole based upon level spacing arguments.<sup>4,6–9,22,25</sup> However, the hole should relax via phonon emission, hence the phonon bottleneck for holes. The absence of a bottleneck for holes suggests a new channel in these colloidal dots (Figure 4d). We proposed the existence of a nonadiabatic relaxation channel mediated by surface ligand vibrations.<sup>8,9</sup> Essentially, ligand vibrations medi-

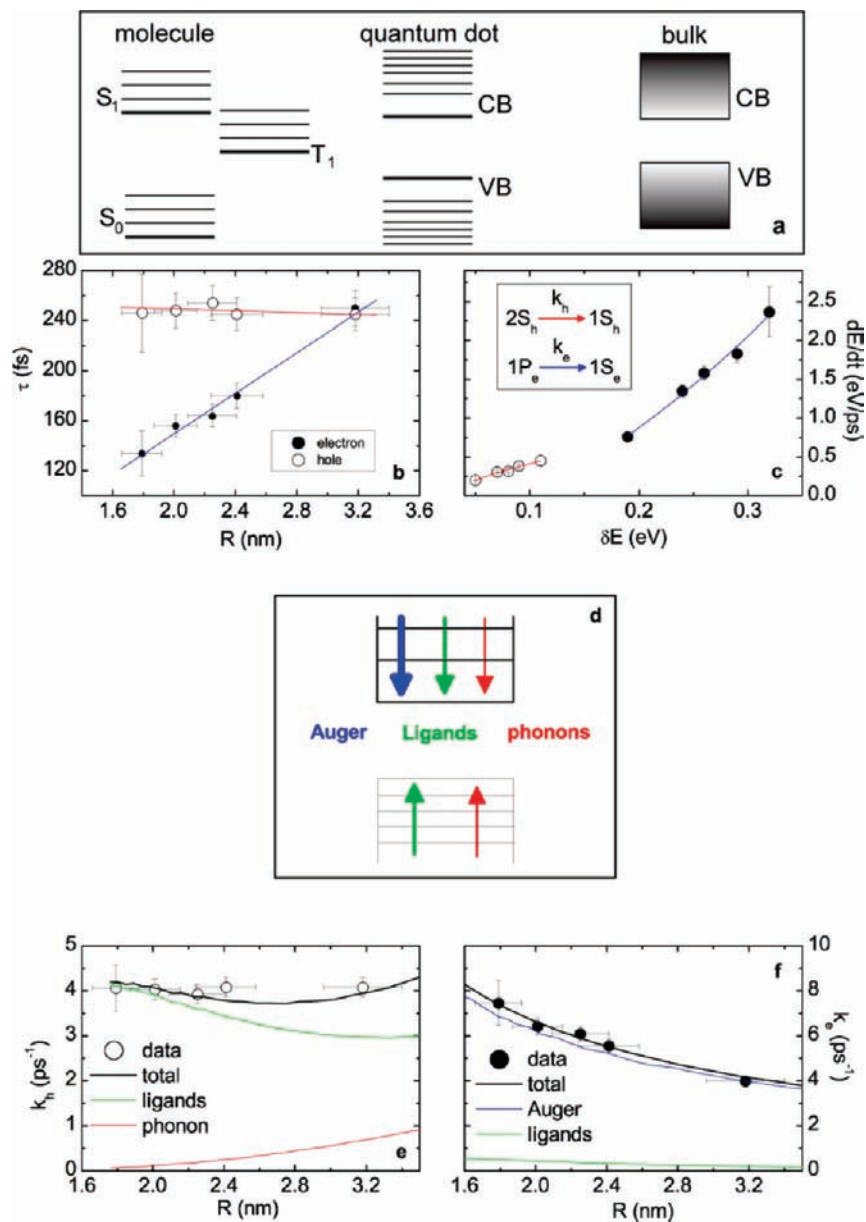


**FIGURE 4.** Hot exciton relaxation dynamics, probed with state-to-state specificity. (a) Schematic of densities of states. (b) Size-dependent electron and hole transition rates. (c) Electron and hole cooling rates vs energy gap. (d) A multichannel picture of hot exciton relaxation pathways. Decomposing the size-dependent hole (e) and electron (f) relaxation pathways.

ate electronic transitions via a breakdown of the Born–Oppenheimer approximation. Our model quantitatively reproduces the experimental trends (Figure 4e,f).

This missing point from this story is the wide variance in measured relaxation rates as well as the large number of theoretical mechanisms which aim to explain the measurements. We propose that the original question of what governs hot carrier relaxation should be modified to a more general question schematically illustrated in Figure 3d: What are the relative contributions of the manifold of relaxation channels to the hot carrier relaxation process and how can these channels be controlled? Essentially, *all* channels can in principle mediate relaxation.

The phonon channel was historically first and hence created the term “phonon bottleneck” and the search thereof. Subsequently, electron–hole channels, exciton–ligand, and exciton–surface channels were proposed. Experimentally, one can prepare situations in which one channel is present and another absent. This situation can obfuscate theoretical interpretation of the experimental results. We proposed a multichannel picture of hot exciton relaxation which is composed of a sum of all possible pathways.<sup>8,9</sup> Hence, all prior results<sup>4,23,24</sup> can be viewed as special cases of the more general *unified* picture of hot exciton relaxation dynamics.

#### 4. Exciton–Exciton Interactions: The Electronic Structure of Biexcitons

Most of the discussions of the electronic structure of quantum dots focus on the *single* exciton (X). This situation is unsurprising, as single excitons are dominantly created under weak excitation conditions. Furthermore, linear optical properties<sup>17,20</sup> (absorption and PL) along with photoconductance are completely determined by the electronic structure of X. However, quantum dots can support multiple excitations *per dot*. Absorption of two photons (or one photon followed by MEG) creates a *biexciton* (XX).<sup>1</sup>

One might expect that the electronic structure of biexcitons is of minor importance, arising only under exotic conditions. However, this view masks the tremendous relevance of biexcitons to a wide variety of situations. For example, optical gain in quantum dots generally arises from stimulated emission (SE) from biexcitons.<sup>1,13,14,26</sup> Similarly, cascaded emission from biexcitons creates (or inhibits) the possibility of creating entangled photon pairs. Finally, the electronic structure of biexcitons is one of the central features in multiple exciton generation<sup>3</sup> and multicarrier recombination,<sup>3,4</sup> yet it has never been experimentally measured.

The simplest parameter with which to characterize the biexciton is its binding energy. The binding energy is the energy difference between twice the energy of X and the energy of XX:  $\Delta_{XX} = 2E_X - E_{XX}$ . While the early experiments on colloidal quantum dots employed non-state-selective pump/probe spectroscopy,<sup>1</sup> the more recent experiments have used time-resolved PL measurements (t-PL).<sup>1,27,28</sup> The advantage of these t-PL measurements is that they yield an unambiguous measurement: the binding energy for the *ground* state of the biexciton. What remains missing from the current work on biexcitons in colloidal quantum dots is a discussion of their electronic structure at the same level as the electronic structure of X.

Our *state-resolved* spectroscopic approach has enabled the observation of fast dynamical processes (excitonic relaxation) and transient parameters (exciton–phonon coupling), ultimately yielding a window into *electronic structural dynamics*. Electronic structural dynamics reflects the transient aspects of structure of excitons as they undergo processes such as generation, relaxation, recombination, and surface trapping. With the requisite resolution in time, frequency, and excitonic state, we are now able to monitor transient species such as excited states of the biexciton.<sup>7,12,16</sup>

Figure 5a,b illustrates how we monitor biexcitons in absorptive (pump/probe) experiments. The pump pulse

populates some excitonic state ( $GS \rightarrow X$ ), and the probe pulse monitors the absorption into the biexciton ( $X \rightarrow XX$ ). Since there is a well-known manifold of excitonic states,<sup>1,2</sup> there must be a manifold of biexcitonics which naturally arises, illustrated in Figure 5a. The energy shifts due to  $\Delta_{XX}$  manifest themselves as changes in the transient absorption spectrum (induced absorptions) to the red of the band edge exciton. Figure 5b shows how this induced absorption arises by parametrizing  $\Delta_{XX}$  relative to the line width ( $\Gamma$ ).

Figure 5c shows representative data upon pumping into the 1P exciton. The time zero signal reflects an excited state of XX comprising a hot electron (1P), and the later time (200 fs) signal corresponds to an excited state consisting of a cold electron (1S) and an Auger up-pumped hole. The signal at late time (2 ps) corresponds to the ground state of the biexciton. Pumping into different initial states yields the binding energies of *specific* biexcitons, as does monitoring the system upon carrier cooling and surface trapping.<sup>12</sup> Figure 5d illustrates the state-resolved binding energies for some of these biexcitons. The differences in these signals at various times (or various initial excitonic states) reflect the *coarse* electronic structure of the biexciton, a point which we will further discuss elsewhere. At present, we focus on the structure of the *band edge biexciton*.

Our pump/probe experiments at low fluence measure absorption from  $X \rightarrow XX$ . These experiments yield binding energies for the ground state biexciton of  $\sim 5\text{--}15$  meV.<sup>12,16</sup> These numbers are not consistent with the t-PL measurements which obtained ground state binding energies of  $\sim 25\text{--}45$  meV (all are size-dependent).<sup>1,27,28</sup> In order to reconcile this discrepancy, we performed pump/probe measurements at high fluence to monitor stimulated emission (SE):  $XX \rightarrow X$ . Under these conditions, we obtained nearly identical results as the t-PL measurements. This situation suggests that there is a fundamentally missing feature in our understanding even of the *ground* state biexciton.

The ground state of the exciton ( $X_1$ ) in Figure 1 is well-known to have an electronic substructure.<sup>1,2</sup> This band edge exciton undergoes degeneracy breaking through electron–hole exchange (fine structure splitting), crystal field splitting, shape asymmetries, and phonon progressions. The sum of these effects gives rise to the observable of the PL Stokes shift for X ( $\delta_X$ ),<sup>20</sup> showing the importance of the excitonic substructure. Our absorptive and emissive experiments on XX show that the biexcitonic states into which the system absorbs and emits are not the same.<sup>16</sup> Hence, there must be electronic *substructure* to the band edge biexc-

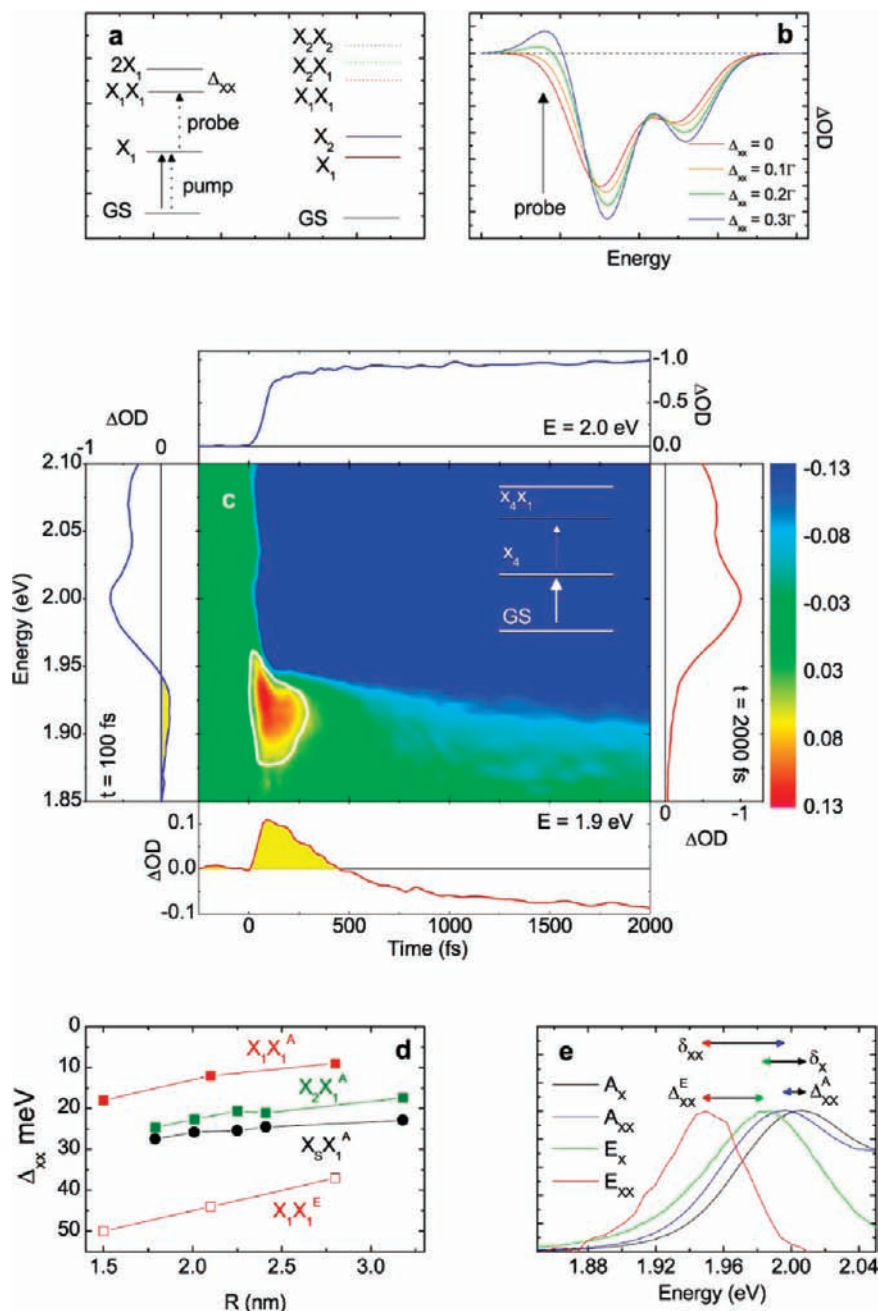


**FIGURE 5.** State-resolved studies of biexcitons. (a) Schematic of the electronic structure of X and XX and the probing via pump/probe spectroscopy. (b) Relating biexciton binding energy to red-edge photoinduced absorptions. (c) Pump/probe data showing the photoinduced absorption upon pumping into the 1P exciton ( $X_4$ ). (d) Energy spectrum of the biexciton in CdSe colloidal quantum dots. The biexciton  $X_iX_j^{A/E}$  denotes a biexciton comprising, for example,  $X_2$  and  $X_1$ . The A/E denotes the absorptive or emissive substate of that biexciton state. (e) Electronic structure of X and XX in terms of Stokes shifts ( $\delta$ ) and binding energies ( $\Delta$ ). The spectra correspond to absorption into X ( $A_x$ ) or XX ( $A_{xx}$ ), and emission from X ( $E_x$ ) or from XX ( $E_{xx}$ ). The binding energies are denoted by whether absorptive (A) or emissive (E) transitions are measured, and the Stokes shifts are denoted by single exciton (X) or biexciton (XX).

citon. This degeneracy breaking in XX is similarly nontrivial, as it creates a unique *biexciton Stokes shift* ( $\delta_{xx}$ ) (Figure 5e). We show below that this previously unobserved biexciton Stokes shift which arises from the structure of XX is in fact the most important parameter governing the physics of optical gain in quantum dots.<sup>13,14</sup>

## 5. Optical Gain

One of the immediate applications of quantum dots is as gain media for optical amplification. The underlying premise is that quantum confinement squeezes the electronic density of states thereby creating transitions with large oscillator strength



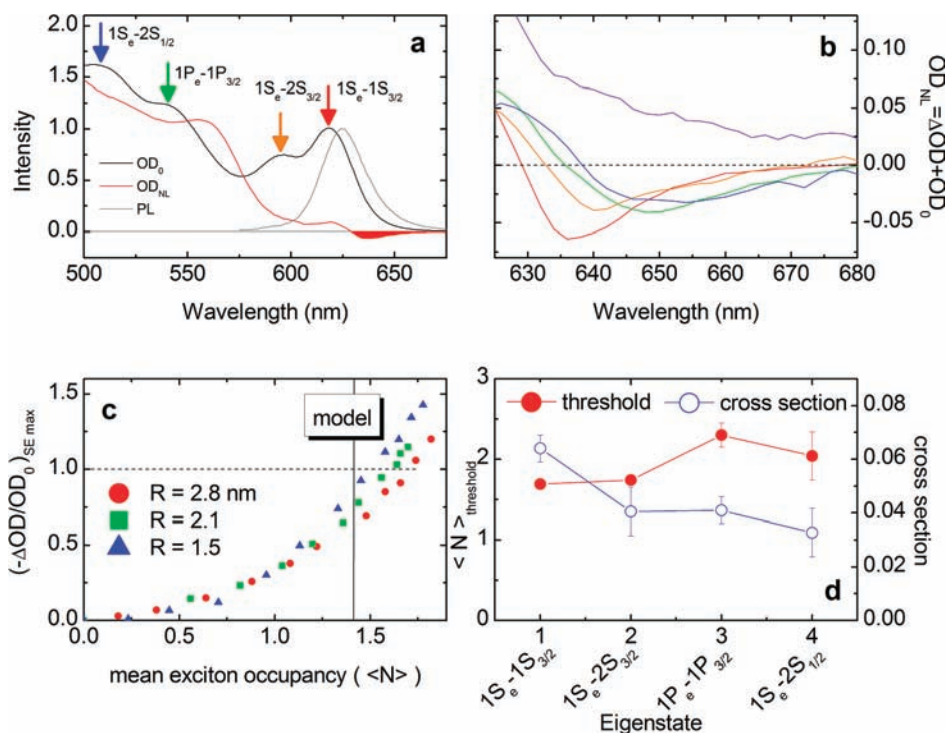


**FIGURE 6.** State-resolved studies of optical gain recovers size independent gain. (a) Illustration of pumping into four initial excitonic states and the presence of optical gain ( $OD_{NL} < 0$ ). (b) Depth and width of the stimulated emission (gain) as a function of initial state. (c) Pumping into  $X_1$  recovers size universal gain. (d) State-dependence to gain metrics of threshold ( $\langle N \rangle_{th}$ ) and cross section ( $\sigma$ ).

and large energy spacings. These conditions should be favorable toward the implementation of such nanostructures into gain media.

The first demonstration of optical gain in these strongly confined colloidal quantum dots was by Klimov and Bawendi.<sup>3</sup> In these early experiments, it was only possible to generate optical gain for dots dispersed in a polymer film, with a strongly size-dependent gain threshold. Klimov subsequently showed optical gain in the native dispersions, but with even more strongly size-dependent thresholds.<sup>29</sup> These gain metrics in solution were found to be strongly sensitive to the passivating ligands as well as the solvent. From these experiments, one might conclude that while optical gain in colloidal quantum dots is possible, it is strongly size-dependent, is environment-dependent, and is neither size universal nor efficient.

Hence, it was expected that the path toward creating nanostructured gain media that are efficient and truly size tunable lay in the development of alternative nanostructures. Initially, quantum rods were developed under the premise that they would have slower multicarrier recombination times thereby enhancing gain lifetimes.<sup>3</sup> An important insight was put forth by Klimov et al. who showed that biexciton interactions could be engineered to lower the gain threshold to below the single exciton level.<sup>26</sup> The rationale was that parasitic excited

state absorption into the biexciton was the factor which blocked gain. By creating a core/shell structure with a Type II band offset, they realized negative biexciton binding energies which created the pathway to single exciton gain media.

In order to explore the physical issues which control optical gain in quantum dots, we applied our state-resolved approach to the phenomenology of gain.<sup>13,14</sup> Our objective was to find the features which can either enable or block the development of optical gain by detailed exploration of the canonical CdSe system. Since gain in CdSe seemed to be strongly dependent upon particle size, ligands, and host matrix, it seemed that there were some key processes which remained elusive. By unraveling the *elementary* processes which govern gain in a prototypical material, one aims to generalize the results to guide a broader inquiry into a long-term goal of creating the *ideal* nanostructured gain material based upon clear design principles.

Figures 6 and 7 summarize the results of our state-resolved optical gain studies. Figure 6a shows the absorption, PL, and nonlinear absorption spectrum of CdSe quantum dots in toluene dispersion. The nonlinear absorption spectrum can be considered as the spectrum of the excited sample ( $OD_{NL} = OD_0 + \Delta OD$ ). Optical gain corresponds to  $OD_{NL} < 0$ , the shaded region in Figure 6a.

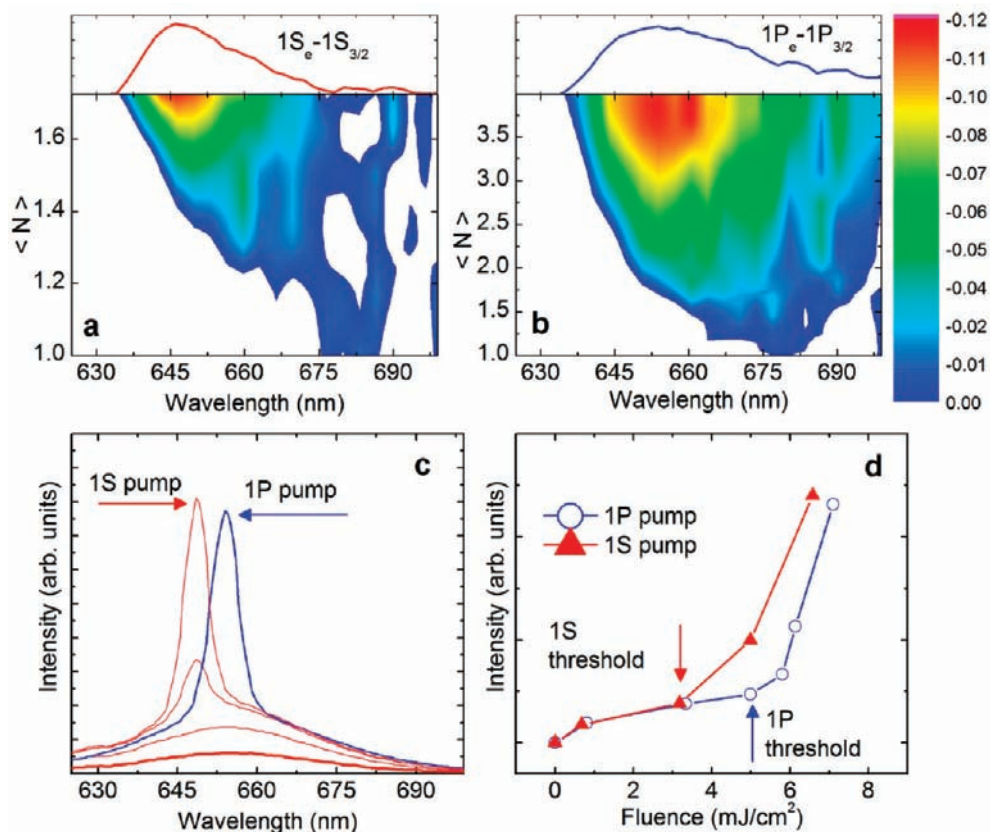


**FIGURE 7.** State-resolved studies of optical gain reveals many-body interactions. Stimulated emission (SE) bandwidth control as a function of exciton concentration for 1S pump (a) and 1P pump (b). The contours correspond to the negative portion of  $(OD_{NL})$ , the SE amplitude. The initial excitonic state-dependence even persists in steady-state amplified spontaneous emission measurements (c and d). This spectral control arises from multiexciton interactions.

One might expect that pumping into different initial excitonic states should have little effect on gain, since the gain measurements are taken well after hot exciton relaxation. Instead, Figure 6b shows that the stimulated emission spectrum (negative portion of  $OD_{NL}$ ) is strongly dependent upon the initial excitonic state.

Recognizing that the largest gain amplitudes were found with band edge excitation ( $X_1$ ), we explored the issue of size-universality maintaining band edge pumping throughout. In contrast to the strong size-dependent gain thresholds previously observed with arbitrary excitation (400 nm), we found that the gain threshold was nearly size-independent as expected from simple modeling (Figure 6c). The gain thresholds we found in colloidal CdSe in toluene are among the lowest ever measured in any material. This result is all the more remarkable considering that the experiments were done using CdSe passivated with ligands and dispersed in solvents which were expected to result in *zero* gain.<sup>29</sup> Clearly, there are underlying dynamical processes at work which are often mistaken as materials issues. The state-dependent thresholds and cross sections are summarized in Figure 6d for one size of dot.

All aspects of the system's gain response are sensitive to the initial excitonic state into which one pumps. The gain phenomenology here<sup>13,14</sup> results directly from three elementary dynamical processes: exciton relaxation,<sup>7-9</sup> surface trapping,<sup>12</sup> and state-specific multiexciton interaction.<sup>7,12,16</sup> Briefly, gain is blocked by parasitic photoinduced absorptions (PAs). The PA arises from biexciton based level shifting which takes on specific values as the system relaxes and ultimately undergoes surface trapping. In some cases, direct excited state surface trapping can compete with intraband relaxation, thereby yielding some aspects of the state-dependent thresholds and cross sections.<sup>13,14</sup>

In addition, we found remarkable qualitative differences based upon the initial excitonic state (Figure 7). Figure 7a,b shows the SE spectra as a function of exciton occupancy for two different initial states: the  $X_1$  exciton ( $1S_e-1S_{3/2}$ ) and the  $X_4$  exciton ( $1P_e-1P_{3/2}$ ). The main observation is the increased gain bandwidth available via excitation into the higher excitonic states. This increased bandwidth does come at a cost of increased threshold and decreased cross section. However, the effect was both prominent and unexpected. Recognizing the

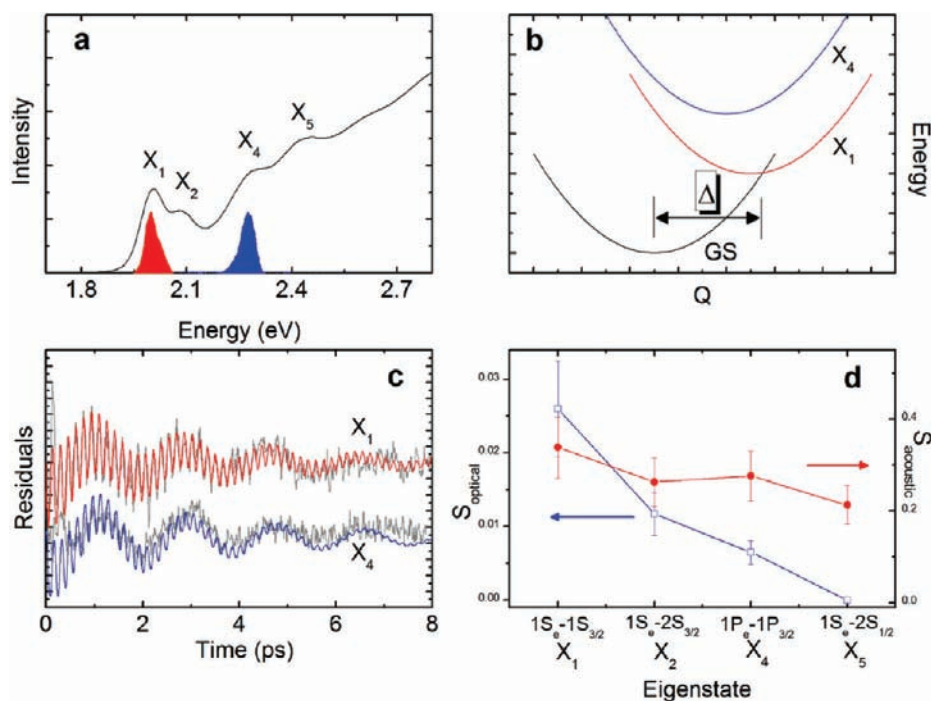


**FIGURE 8.** Exciton–phonon coupling with specificity to the manifold of quantized excitonic states. (a) Representative absorption spectrum and pump spectra. (b) Representation of state-specific coupling strengths using the displaced harmonic oscillator model. (c) Real time observation of coherent optical and acoustic phonons. (d) State-resolved couplings.

electron degeneracies are two and six, respectively, we assigned the increased bandwidth with 1P excitation to stimulated emission from higher multiexcitons.<sup>13,14</sup> Thus, the ability to control the gain bandwidth arises from the level shiftings due to specific multiexcitons (XX, XXX, etc.).<sup>7,12,16</sup> This ability to control bandwidth via multiexciton interactions is likely unique to these strongly confined quantum dots. Finally, we note that this spectral tuning by initial excitonic state persists even for continuous wave (CW) measurements of amplified spontaneous emission (Figure 7c,d).

## 6. Exciton–Phonon Interactions

The mechanism of how the excitons couple to the lattice is one of the oldest topics in quantum dot science.<sup>30–33</sup> The lattice vibrations (phonons) are coupled to the electronic states (excitons) through various forms of exciton–phonon coupling: Fröhlich, deformation potential, and piezoelectricity. The two families of vibrational modes are low frequency acoustic phonons ( $\sim 20 \text{ cm}^{-1}$ ) and higher frequency optical phonons ( $\sim 200 \text{ cm}^{-1}$ ), for CdSe.

The strength of coupling between the excitonic states and the phonon modes is of great importance. In terms of basic science, exciton–phonon coupling provides a ruler for assessing the extent to which the wave functions of the dot are truly known. The general mechanisms of electron–phonon coupling in bulk crystals is well understood. The main problem

becomes one of assessing whether the computed wave functions closely resemble the true wave functions. Hence, a measurement of these couplings provides a critical test of theory. In addition, the strength of coupling is of great importance to quantum dot based devices. The phonon modes can play a role in hot carrier relaxation processes, determine the homogeneous linewidths for nonlinear optical devices, and relate to heat dissipation and piezoelectric response.

There has been a large body of theoretical work which has predicted all permutations of size-dependences for both the optical and acoustic modes. The divergences of the theories suggests the difficulty in computing realistic excitonic wave functions. Unfortunately, the experimental results had been equally divergent.<sup>20,30,31,33,34</sup> In general, the frequency domain experiments see enormous coupling to the optical modes but do not detect the acoustic modes. In contrast, the time domain experiments have seen the optical modes or the acoustic modes, but not both (in the case of CdSe).

In order to explore these puzzling discrepancies, we applied our state-resolved spectroscopic approach toward the issue of exciton–phonon coupling in quantum dots.<sup>10,11</sup> In our experiments, we tuned a femtosecond pump pulse to specific excitonic states (Figure 8a) and monitored the change in transmission of the probe pulse, tuned to a point in the absorption spectrum which maximizes the oscillation amplitude (the  $A_1$  spectral feature). The oscillation amplitudes can

be directly converted to coupling strengths via the standard displaced harmonic oscillator model (Figure 8b). The data are shown in Figure 8c.

Upon direct excitation into the band edge exciton, our experiments yielded the first *simultaneous* observation of coherent optical and acoustic phonons in CdSe quantum dots.<sup>10,11</sup> Both are of nearly equal amplitude, but the acoustic mode is more strongly coupled. The more interesting point is that our experiments yield the first observation of the *state-dependence* of the exciton–phonon couplings.<sup>10,11</sup> We find that the coupling to the optical mode drops off rapidly as one moves to higher excitonic states, whereas the acoustic mode is less strongly dependent upon state. Our Raman measurements are consistent with the early frequency domain results<sup>33,34</sup> in that we find that resonance Raman yields couplings which are completely *inconsistent* with the time domain results.

The state-dependence to the exciton–phonon couplings<sup>10,11</sup> suggests a rationalization for this discrepancy. Each experiment may not measure the same states. Time domain measurements without state-selectivity simply excited into high-lying states with weak coupling to optical phonons. In contrast, the frequency domain experiments are sensitive to the accumulation of charges *during the course* of the experiment, a point made earlier by Wise.<sup>31</sup> Hence, the frequency domain experiments most likely do not measure the coupling to the intrinsic excitonic state, but one that is contaminated by charge accumulation at the surface. These excitonic-state-dependent studies of exciton–phonon coupling reveal that each state is uniquely coupled to each phonon mode. This point is perhaps unsurprising. However, the result is important in reconciling a divergent experimental literature which has failed to perform the anticipated feedback for difficult calculations.

## 7. Summary and Outlook

In this Account, we have provided an overview of some of the main issues which represent the core of the science behind semiconductor quantum dots. We employ the term *excitons* to refer to the electronic structure, dynamics, and phenomenology of excitons in these materials. These fundamental investigations into the elementary dynamical processes of excitons in quantum dots ultimately aim to produce a detailed picture of the workings of the dot. Such an understanding is essential toward the rational implementation of these materials into devices. While the work discussed here is on colloidal CdSe quantum dots, these results are not to be viewed in isolation. The investigations into this canonical system should

establish the methods of analysis for all classes of nanoscale semiconductors.

*The author is indebted to an excellent group of students who built the lab and performed the experiments described here. Financial support from NSERC and CFI is acknowledged.*

**Note Added after ASAP.** This paper was posted to the web on October 13, 2010 with a typographical error in part C of Figure 6. The revised version was posted on October 22, 2010.

---

### BIOGRAPHICAL INFORMATION

**Patanjali Kambhampati** received a B.A. in Chemistry from Carleton College in 1992 and a Ph.D. in Chemistry from the University of Texas at Austin in 1998. His doctoral work focused on ultrahigh vacuum surface studies of adsorbate–substrate charge transfer excitations and surface enhanced Raman scattering under the supervision of Alan Campion. From 1999 to 2001, he was a Postdoctoral Associate with Paul Barbara, also at the University of Texas at Austin. His postdoctoral work focused on femtosecond laser spectroscopy of condensed phase chemical dynamics of the solvated electron and intramolecular electron transfer. From 2001 to 2003, he was involved in early phase work in a fiber optic startup based in Los Angeles. At McGill University, where his group focuses on ultrafast dynamics in quantum dots, he was an Assistant Professor from 2003 to 2009 and is presently an Associate Professor.

---

### FOOTNOTES

\*E-mail: pat.kambhampatimcgill.ca.

---

### REFERENCES

- Klimov, V. I. Spectral and dynamical properties of multielectrons in semiconductor nanocrystals. *Annu. Rev. Phys. Chem.* **2007**, *58*, 635–673.
- Efros, A. L.; Rosen, M. The electronic structure of semiconductor nanocrystals. *Annu. Rev. Mater. Sci.* **2000**, *30*, 475–521.
- Klimov, V. I. Mechanisms for photogeneration and recombination of multielectrons in semiconductor nanocrystals: Implications for lasing and solar energy conversion. *J. Phys. Chem. B* **2006**, *110*, 16827–16845.
- Klimov, V. I. Optical Nonlinearities and Ultrafast Carrier Dynamics in Semiconductor Nanocrystals. *J. Phys. Chem. B* **2000**, *104*, 6112–6123.
- Brus, L. E. A simple model for the ionization potential, electron affinity, and aqueous redox potentials of small semiconductor crystallites. *J. Chem. Phys.* **1983**, *79*, 5566–5571.
- Nozik, A. J. Spectroscopy and hot electron relaxation dynamics in semiconductor quantum wells and quantum dots. *Annu. Rev. Phys. Chem.* **2001**, *52*, 193–231.
- Sewall, S. L.; Cooney, R. R.; Anderson, K. E. H.; Dias, E. A.; Kambhampati, P. State-to-state exciton dynamics in semiconductor quantum dots. *Phys. Rev. B* **2006**, *74*, 235328.
- Cooney, R. R.; Sewall, S. L.; Anderson, K. E. H.; Dias, E. A.; Kambhampati, P. Breaking the Phonon Bottleneck for Holes in Semiconductor Quantum Dots. *Phys. Rev. Lett.* **2007**, *98*, 177403–4.
- Cooney, R. R.; Sewall, S. L.; Dias, E. A.; Sagar, D. M.; Anderson, K. E. H.; Kambhampati, P. Unified picture of electron and hole relaxation pathways in semiconductor quantum dots. *Phys. Rev. B* **2007**, *75*, 245311–14.
- Sagar, D. M.; Cooney, R. R.; Sewall, S. L.; Dias, E. A.; Barsan, M. M.; Butler, I. S.; Kambhampati, P. Size dependent, state-resolved studies of exciton-phonon couplings in strongly confined semiconductor quantum dots. *Phys. Rev. B* **2008**, *77*, 235321–14.

- 11 Sagar, D. M.; Cooney, R. R.; Sewall, S. L.; Kambhampati, P. State-Resolved Exciton-Phonon Couplings in CdSe Semiconductor Quantum Dots. *J. Phys. Chem. C* **2008**, *112*, 9124–9127.
- 12 Sewall, S. L.; Cooney, R. R.; Anderson, K. E. H.; Dias, E. A.; Sagar, D. M.; Kambhampati, P. State-resolved studies of biexcitons and surface trapping dynamics in semiconductor quantum dots. *J. Chem. Phys.* **2008**, *129*, 084701.
- 13 Cooney, R. R.; Sewall, S. L.; Sagar, D. M.; Kambhampati, P. Gain Control in Semiconductor Quantum Dots via State-Resolved Optical Pumping. *Phys. Rev. Lett.* **2009**, *102*, 127404–4.
- 14 Cooney, R. R.; Sewall, S. L.; Sagar, D. M.; Kambhampati, P. State-Resolved Manipulations of Optical Gain in Semiconductor Quantum Dots: Size Universality, Gain Tailoring, and Surface Effects. *J. Chem. Phys.* **2009**, *131*, 164706.
- 15 Sewall, S. L.; Cooney, R. R.; Kambhampati, P. Experimental tests of effective mass and atomistic approaches to quantum dot electronic structure: Ordering of electronic states. *Appl. Phys. Lett.* **2009**, *94*, 243116–3.
- 16 Sewall, S. L.; Franceschetti, A.; Cooney, R. R.; Zunger, A.; Kambhampati, P. Direct observation of the structure of band-edge biexcitons in colloidal semiconductor CdSe quantum dots. *Phys. Rev. B* **2009**, *80*, 081310(R).
- 17 Norris, D. J.; Bawendi, M. G. Measurement and assignment of the size-dependent optical spectrum in CdSe quantum dots. *Phys. Rev. B* **1996**, *53*, 16338–16346.
- 18 Franceschetti, A.; Zunger, A. Direct pseudopotential calculation of exciton Coulomb and exchange energies in semiconductor quantum dots. *Phys. Rev. Lett.* **1997**, *78*, 915–918.
- 19 Prezhdo, O. V. Photoinduced Dynamics in Semiconductor Quantum Dots: Insights from Time-Domain ab Initio Studies. *Acc. Chem. Res.* **2009**, *42*, 2005–2016.
- 20 Norris, D. J.; Efros, A. L.; Rosen, M.; Bawendi, M. G. Size dependence of exciton fine structure in CdSe quantum dots. *Phys. Rev. B* **1996**, *53*, 16347–16354.
- 21 Wang, L.-W.; Zunger, A. High-Energy Excitonic Transitions in CdSe Quantum Dots. *J. Phys. Chem. B* **1998**, *102*, 6449–6454.
- 22 Efros, A. L.; Kharchenko, V. A.; Rosen, M. Breaking the phonon bottleneck in nanometer quantum dots: role of Auger-like processes. *Solid State Commun.* **1995**, *93*, 281–284.
- 23 Pandey, A.; Guyot-Sionnest, P. Slow Electron Cooling in Colloidal Quantum Dots. *Science* **2008**, *322*, 929–932.
- 24 Guyot-Sionnest, P.; Wehrenberg, B.; Yu, D. Intraband relaxation in CdSe nanocrystals and the strong influence of the surface ligands. *J. Chem. Phys.* **2005**, *123*, 074709/1–074709/7.
- 25 Wang, L.-W.; Califano, M.; Zunger, A.; Franceschetti, A. Pseudopotential Theory of Auger Processes in CdSe Quantum Dots. *Phys. Rev. Lett.* **2003**, *91*, 056404/1–056404/4.
- 26 Klimov, V. I.; Ivanov, S. A.; Nanda, J.; Achermann, M.; Bezel, I.; McGuire, J. A.; Piryatinski, A. Single-exciton optical gain in semiconductor nanocrystals. *Nature* **2007**, *447*, 441–446.
- 27 Bonati, C.; Mohamed, M. B.; Tonti, D.; Zgrablic, G.; Haacke, S.; van Mourik, F.; Chergui, M. Spectral and dynamical characterization of multiexcitons in colloidal CdSe semiconductor quantum dots. *Phys. Rev. B* **2005**, *71*, 205317.
- 28 Caruge, J. M.; Chan, Y.; Sundar, V.; Eisler, H. J.; Bawendi, M. G. Transient photoluminescence and simultaneous amplified spontaneous emission from multiexciton states in CdSe quantum dots. *Phys. Rev. B* **2004**, *70*, 085316.
- 29 Malko, A. V.; Mikhailovsky, A. A.; Petruska, M. A.; Hollingsworth, J. A.; Klimov, V. I. Interplay between Optical Gain and Photoinduced Absorption in CdSe Nanocrystals. *J. Phys. Chem. B* **2004**, *108*, 5250–5255.
- 30 Krauss, T. D.; Wise, F. W. Coherent Acoustic Phonons in a Semiconductor Quantum Dot. *Phys. Rev. Lett.* **1997**, *79*, 5102–5105.
- 31 Wise, F. W. Lead Salt Quantum Dots: the Limit of Strong Quantum Confinement. *Acc. Chem. Res.* **2000**, *33*, 773–780.
- 32 Mittleman, D. M.; Schoenlein, R. W.; Shiang, J. J.; Colvin, V. L.; Alivisatos, A. P.; Shank, C. V. Quantum size dependence of femtosecond electronic dephasing and vibrational dynamics in CdSe nanocrystals. *Phys. Rev. B* **1994**, *49*, 14435–14447.
- 33 Alivisatos, A. P.; Harris, T. D.; Carroll, P. J.; Steigerwald, M. L.; Brus, L. E. Electron-vibration coupling in semiconductor clusters studied by resonance Raman spectroscopy. *J. Chem. Phys.* **1989**, *90*, 3463–3468.
- 34 Empedocles, S. A.; Neuhäuser, R.; Shimizu, K.; Bawendi, M. G. Photoluminescence from single semiconductor nanostructures. *Adv. Mater.* **1999**, *11*, 1243–1256.